AFCEC-CX-TY-TR-2016-0007

HANDHELD CHEM/BIOSENSOR USING EXTREME CONFORMATIONAL CHANGES IN DESIGNED BINDING PROTEINS TO ENHANCE SURFACE PLASMON RESONANCE (SPR) (AUTHORS' FINAL VERSION)

Lori A. Lepak and Igor Bendoym
Phoebus Optoelectronics LLC, 54 West 40th Street, New York, NY 10018

Peter Schnatz and Derek Kosciolek
The City College of New York, 419 Marshak Science Bldg, 160 Convent Ave., New York, NY 10031

Ronald Kroder
Phoebus Optoelectronics LLC, 54 West 40th Street, New York, NY 10018 &
The City College of New York, 419 Marshak Science Bldg, 160 Convent Ave., New York, NY 10031

David T. Crouse
Phoebus Optoelectronics LLC, 54 West 40th Street, New York, NY 10018 &
the Department of Electrical and Computer Engineering, Clarkson University, PO Box 5720, Potsdam, NY 13699

Contract No. FA4819-16-C-0001

April 2016

AIR FORCE CIVIL ENGINEER CENTER
READINESS DIRECTORATE

■ **Requirements & Acquisition Division** ■ **United States Air Force** ■ **Tyndall Air Force Base, FL 32403-5323**

DISCLAIMER

Reference herein to any specific commercial product, process, or service by trade name, trademark, manufacturer, or otherwise does not constitute or imply its endorsement, recommendation, or approval by the United States Air Force. The views and opinions of authors expressed herein do not necessarily state or reflect those of the United States Air Force.

This report was prepared as an account of work sponsored by the United States Air Force. Neither the United States Air Force, nor any of its employees, makes any warranty, expressed or implied, or assumes any legal liability or responsibility for the accuracy, completeness, or usefulness of any information, apparatus, product, or process disclosed, or represents that its use would not infringe privately owned rights.

REPORT DOCUMENTATION PAGE

Form Approved
OMB No. 0704-0188

PLEASE DO NOT RETURN YOUR FORM TO THE ABOVE ADDRESS.

1. REPORT DATE *(DD-MM-YYYY)*	2. REPORT TYPE	3. DATES COVERED *(From - To)*
03/24/2016	Abstract	08/14/2015--03/31/2016

4. TITLE AND SUBTITLE

Handheld chem/biosensor using extreme conformational changes in designed binding proteins to enhance surface plasmon resonance (SPR) (AUTHOR'S FINAL VERSION)

5a. CONTRACT NUMBER

FA4819-16-C-0001

5b. GRANT NUMBER

5c. PROGRAM ELEMENT NUMBER

6. AUTHOR(S)

*Lori A. Lepak, ^Peter Schnatz, *Igor Bendoym, ^Derek Kosciolek, *^Ronald Koder, *%David T Crouse

5d. PROJECT NUMBER

5e. TASK NUMBER

5f. WORK UNIT NUMBER

7. PERFORMING ORGANIZATION NAME(S) AND ADDRESS(ES)

*Phoebus Optoelectronics LLC, 54 West 40th Street, New York, NY 10018; ^The City College of New York, 419 Marshak Science Bldg, 160 Convent Ave., New York, NY 10031; %Department of Electrical and Computer Engineering, Clarkson University, PO Box 5720, Potsdam, NY 13699

8. PERFORMING ORGANIZATION REPORT NUMBER

9. SPONSORING/MONITORING AGENCY NAME(S) AND ADDRESS(ES)

Air Force Civil Engineer Center
Readiness Directorate
Requirements and Acquisition Division
139 Barnes Drive, Suite 1
Tyndall Air Force Base, FL 32403-5323

10. SPONSOR/MONITOR'S ACRONYM(S)

AFCEC/CXA

11. SPONSOR/MONITOR'S REPORT NUMBER(S)

AFCEC-CX-TY-TP-2016-0007

12. DISTRIBUTION/AVAILABILITY STATEMENT

Distribution A: Approved for public release; distribution unlimited.

13. SUPPLEMENTARY NOTES

Ref Public Affairs Case # AFCEC-201608, 27 April 2016. Document contains color images. Presented at the SPIE Defense + Commercial Sensing Conference held in Baltimore, Maryland on 17-21 April 2016.

14. ABSTRACT

We propose the development of a highly sensitive handheld chem/biosensor device using a novel class of engineered proteins, designed to undergo extreme conformational changes upon binding their target, which in turn cause extreme changes in refractive index in the protein layer. These proteins are attached to a detector chip with a structured metasurface, to translate the refractive index change into an enhanced shift in surface plasmon resonances (SPR), thereby improving the sensitivity of the overall detector relatively to current commercially available SPR systems. Theoretical calculations have demonstrated the potential of the conformational changes in the engineered proteins to provide the desired change in refractive index. A plasmonic chip with a simple grating metasurface structure has been designed to maximize the SPR shift, and a prototype chip has been fabricated. A prototype for the overall device housing has also been fabricated, and all other required optical components, which are commercially available, have been assembled. This proposed device holds considerable promise as a low-cost, highly sensitive, field-deployable detection system for chemical and biological toxins.

15. SUBJECT TERMS

Surface Plasmon Resonance (SPR), protein design, protein engineering, supercharged protein, metamaterials, metasurfaces, biosensor, chemical sensor

16. SECURITY CLASSIFICATION OF:			17. LIMITATION OF ABSTRACT	18. NUMBER OF PAGES	19a. NAME OF RESPONSIBLE PERSON
a. REPORT	b. ABSTRACT	c. THIS PAGE			JOSEPH WANDER
U	U	U	SAR	13	19b. TELEPHONE NUMBER *(Include area code)*

Reset

Handheld chem/biosensor using extreme conformational changes in designed binding proteins to enhance surface plasmon resonance (SPR)

Lori A. Lepak*[a], Peter Schnatz[b], Igor Bendoym[a], Derek Kosciolek[b], Ronald Koder[a,b], David T Crouse [a,c]

[a]Phoebus Optoelectronics LLC, WeWork, 54 West 40th Street, New York, NY 10018; [b]The City College of New York, 419 Marshak Science Bldg., 160 Convent Ave., New York, NY 10031; [c]Department of Electrical and Computer Engineering, Clarkson University, PO Box 5720, Potsdam, NY 13699

*lorilepak@gmail.com; phone 1 315 224-1190; www.phoebusopto.com

ABSTRACT

We present research results centered on development of a highly sensitive handheld chem/biosensor device using a novel class of engineered proteins, designed to undergo extreme conformational changes upon binding their target, which in turn cause extreme changes in refractive index in the protein layer. These proteins are attached to a detector chip with a structured metasurface, to translate the refractive index change into an enhanced shift in surface plasmon resonances (SPR), thereby improving the sensitivity of the overall detector relatively to current commercially available SPR systems. Theoretical calculations have demonstrated the potential of the conformational changes in the engineered proteins to provide the desired change in refractive index. A plasmonic chip with a simple grating metasurface structure was designed to maximize the SPR shift. A prototype chip and a prototype for the overall device housing were fabricated with the inclusion of all other required (commercially available) optical components. The proposed device holds considerable promise as a low-cost, highly sensitive, field-deployable detection system for chemical and biological toxins.

Keywords: Surface Plasmon Resonance (SPR), protein design, protein engineering, supercharged protein, metamaterials, metasurfaces, biosensor, chemical sensor

1. INTRODUCTION

1.1 Proposed biosensor device

The overall objective of this project is to create a low-cost, high-sensitivity, rapid-sensing platform for the detection and identification of biological toxins—a hand-held plasmonic biosensor device. As discussed in detail below, this sensor device incorporates a new class of designed, supercharged proteins, bound to a detector chip with a highly structured metasurface, to enhance the shift in surface plasmon resonances (SPR), thereby improving the sensitivity of the overall detector. The proposed device achieves several significant improvements over existing SPR biosensing instruments, including:

1. Increased Sensitivity: The system employs a new class of designed proteins with extraordinarily large conformational changes upon analyte binding, producing an orders-of-magnitude increase in sensitivity.

2. Robustness and compactness: All the optical components of the system are in line with each other, making for an easier, more robust, and more stable alignment than existing reflection-based systems.

3. Low-cost, multi-functional: The biosensing chip is planar (i.e., flat), cheap, disposable, and quickly interchangeable, allowing for multiple and repeated testing for different toxins in the field (e.g., battlefield, ports-of-entry, first responders …)

The overall system operates by detecting changes in the transmitted light, rather than reflected light,that occur with the binding of a particular toxin to the functionalized surface. The initial, 3D-printed prototype housing of the device

is shown in Figure 1. Figure 1 (left) shows one half of the complete, 3D-printed custom-designed housing for the module, including a slide-in tray that holds the plasmonic chip and sample to be tested. In this initial prototype, the sample wafer sits on a tray with an exposed underside to allow light to pass through it. A narrow-bandwidth light source illuminates the plasmonic biosensor chip from below, exciting plasmon modes on the chip. Any binding event of a biotoxin will alter the transmission through the chip, as measured by the photodiode array above. This geometry allows all the optical components to be in line with each other, making for an inherently more-compact and -robust system. These innovations form the basis of a transmission-based device with an easily replicable disposable sensing chip. Figure 1 (right) shows the real-sized housing with many of the components inserted into it. From to top, the added components are: 850-nm, 10-mW laser diode, 4.51-mm aspheric collimating lens, linear polarizer, (tray), 5.1-mm^2-active-area silicon photodetector. The extra spaces along the top, bottom, and side are intended to house batteries and circuitry. During actual operation, the lens will sit in the gap directly below where it is currently pictured.

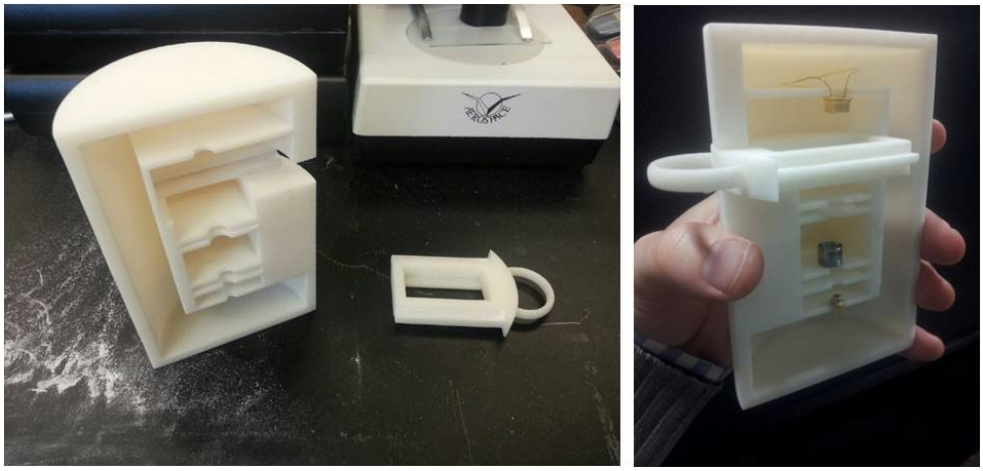

Figure 1. Completed 3D printed module Left: the actual-size housing/casing immediately after 3D printing. Right: optical components (from bottom to top: laser diode, collimating lens, polarizer, and photodetector) inserted into the module.

1.2 Engineered binding proteins

Biosensors employing surface plasmon resonance (SPR) spectroscopy often use rigid structures, such as antibodies, as stationary ligands to detect the presence of small molecules that they bind[1]. This method typically detects a change in surface refractive index upon binding of 0.0001 – 0.001. We propose that a dynamic ligand that undergoes a conformational phase change upon binding will enhance this signal. Analyte-induced folding of intrinsically disordered proteins (IDPs) may offer an opportunity to improve the response of SPR spectroscopy.

IDPs have been found to be essential in cell biology, playing important roles in signal transduction and regulatory functions.[2,3] Their functional dependence on a native unstructured state at physiological conditions has catalyzed a rapid increase in studies regarding IDP behavior. It has been shown that this class of proteins is completely unstructured or contains unstructured regions until an environmental signal or binding event occurs[4]. Our interests lie in the rational design of IDPs which exhibit coupled folding and binding behavior; we believe a large conformational change upon binding to a target analyte will cause enhanced local changes in the refractive index.

The goal is to use emergent computational techniques[5,6,7] to identify or design natural or artificial IDPs that undergo a significant phase transition from a predominantly rigid coil to an ordered, folded structure upon analyte binding. Past studies on the amino acid sequences of IDPs have reported that a large net charge[8,9,10,11] and reduced hydrophobicity[8,9,11] can impart instability and result in a natively unfolded state at neutral pH. We plan to mimic these effects, focusing on incorporating high net charge by mutating the solvent exposed side chains of neutral proteins to basic residues. The electrostatic repulsion of the negative charges will destabilize the structure and force it to take on characteristics similar to a random coil conformation. By increasing the solution ionic strength it is possible to screen the side chain charges and reduce the repulsive forces, switching the energetically favorable conformation from

random coil to natively folded. Similarly, the addition of analyte will induce folding at an experimentally determined ionic strength, exhibiting the desired IDP behavior.

1.3 Surface plasmon resonance (SPR) and metasurfaces

Extraordinary optical transmission (EOT) through subwavelength apertures was first observed by T.W. Ebbesen in 1998.[12] His article in *Nature*, which described exceptional optical characteristics of metallic thin films perforated with subwavelength-sized apertures, spawned the research field of metamaterials and anomalous transmission. Ebbesen observed that anomalously large amounts of light were transmitted through subwavelength apertures, far in excess of the predictions of conventional aperture theory. He hypothesized that the excess transmission was mediated by surface plasmons (SPs).

The proposed device utilizes surface plasmonic effects to create more-sensitive detection capabilities in the proposed transmission-based apparatus. The device incorporates a disposable, nanofabricated plasmonic chip (a metal–glass–semiconductor composite), in which the components are arranged in a metasurface structure—a highly organized, and periodically repeating pattern, with feature sizes on the scale of several hundred nanometers. In general, metasurface patterns can be simple grids, arrays of holes in a metal film, or more complex designs such as concentric circles or ellipses. By using a combination of proprietary software and commercial photonics packages to model the optical properties of these materials, the shapes of the patterns and the chemical composition of the component materials may be chosen to achieve the desired light-controlling behavior. For simplicity, nanopatterned grating structures with high depth-to-width ratios were chosen to transmit narrow wavelength ranges of light. These transmission bands shift in response to analyte binding of the detector proteins, as the engineered extreme change in protein conformation induces an extreme change in the index of refraction at the chip surface. The metasurface structure is designed to induce a detectable shift (ideally >20 nm) in the transmission peak.

2. METHODS

2.1 Protein conformation and refractive index

Because several of our preliminary measurements of the effect of the conformational changes of the designed proteins upon refractive index were performed in reflection mode, our initial analysis assumed the optics are in the Kretschmann configuration[13] (Figure 2), although, as discussed below, these results ultimately prove to be independent of geometry,

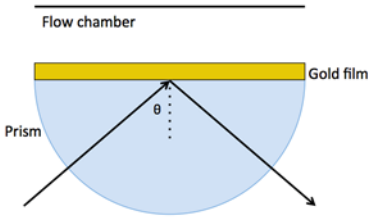

Figure 2. Surface plasmon resonance spectroscopy schematic. The laser passes through the prism and is incident on the gold film at angle θ. The angle at which SPR resonance is achieved will exhibit a significant reduction in reflectance.

allowing us to consider other optical configurations, including transmission mode.) The Kretschmann arrangement contains a gold film at varying angles. If the angle satisfies the dispersion relation for the three-layer system, the light will be absorbed and excite surface plasmons in the metal. Consequently, the reflectance will be reduced at that resonance angle. The reflectance can be computed as a function of incident angle by repeated application of the Fresnel equation. A gold film of thickness d_g has the following ray transfer matrix:

$$\boldsymbol{M} = \begin{bmatrix} \cos(k_{yg} d_g) & -\frac{i\epsilon_g}{k_{yg}} \sin(k_{yg} d_g) \\ -\frac{i k_{yg}}{\epsilon_g} \sin(k_{yg} d_g) & \cos(k_{yg} d_g) \end{bmatrix}.$$

Here, the *y*-component of the wave vector, k_{yg}, passing through the gold film can be determined from the incident angle, θ_i, and the incident wavelength, λ, at the gold–prism interface

$$k_{yg}^2 = n_p^2 \left(\frac{2\pi}{\lambda}\right)^2 \left(\frac{n_g^2}{n_p^2} - \sin^2 \theta_i\right),$$

where n_g and n_p are the refractive indices of the gold and prism, respectively. The reflection coefficient, $r_p(\theta_i)$, is given by

$$r(\theta_i) = \frac{\left(M_{11} + M_{12} \frac{k_{ys}}{\epsilon_s}\right) \frac{k_{yp}}{\epsilon_p} - \left(M_{21} + M_{22} \frac{k_{ys}}{\epsilon_s}\right)}{\left(M_{11} + M_{12} \frac{k_{ys}}{\epsilon_s}\right) \frac{k_{yp}}{\epsilon_p} + \left(M_{21} + M_{22} \frac{k_{ys}}{\epsilon_s}\right)}.$$

The wave vectors in the prism and the sample are denoted k_{yp} and k_{ys}, respectively. Like k_{yg}, they are defined by the incident angle and the refractive indices of the configuration components:

$$k_{yp}^2 = n_p^2 \left(\frac{2\pi}{\lambda}\right)^2 \cos^2 \theta_i$$

$$k_{ys}^2 = n_p^2 \left(\frac{2\pi}{\lambda}\right)^2 \left(\frac{n_s^2}{n_p^2} - \sin^2 \theta_i\right),$$

where n_s is the refractive index of the sample just above the gold film in the flow chamber (Figure 1). Finally, the reflectance as a function of incident angle is given by

$$R(\theta_i) = |r(\theta_i)|^2$$

Since the dielectric constant and the refractive index are intimately related ($n = \sqrt{\epsilon}$) any change to the refractive index at the surface of the gold film in the sample chamber will cause a shift in the angle of minimum reflectance. A typical reflectance spectrum for the parameters in Table 1 is depicted in Figure 3.

Parameter	Value
n_p	1.517
ϵ_p	2.301
n_g	0.19591
ϵ_g	$-10.575 + i1.2765$
n_s	1.33
ϵ_s	1.7689
d_m	60 nm
λ	633 nm

Table 1. Parameters for reflectance spectrum shown in Figure 2.

Here the minimum angle of reflectance is 64.06°; this angle varies linearly with the refractive index of the sample n_s (Figure 3, insert). The slope of a fitted line to this plot is 95.35, indicating that for an increase in refractive index of 0.1, there is a minimum reflectance angle shift of 9.535°. Furthermore, due to the relative refractive indices of the three mediums, the wave passing into the sample chamber is, in fact, an evanescent wave with penetration depth $1/k_{ys}$.

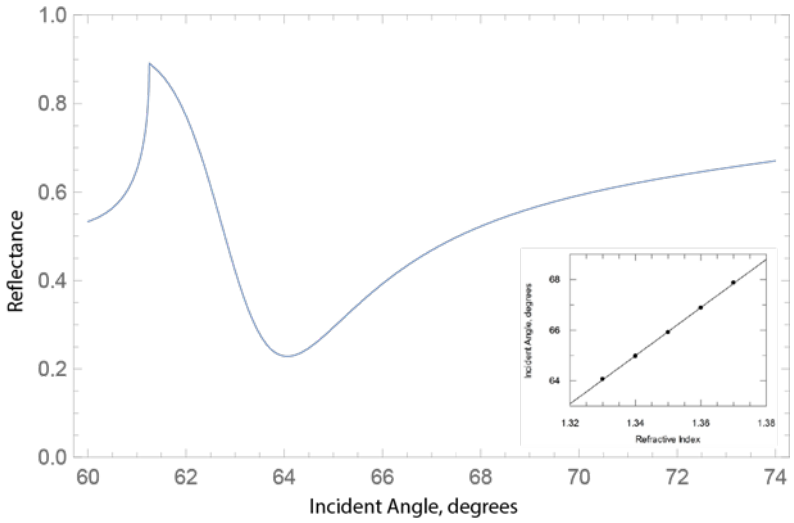

Figure 3. Reflectance spectra for parameters set in Table 1.

The presence of supercharged IDPs on the surface of the gold will induce a binding-dependent refractive index at the gold–sample interface. After binding to the target analyte, the protein will undergo a large conformational change that will affect the refractive index of the sample just above the gold surface. To determine the magnitude of this change, we will estimate the refractive index of our protein using a method outlined by McMeekin et al[14,15]. The refraction per gram of protein, R_{p}, is calculated as the mass-weighted average of the refraction per gram of the contributing amino acids R_a,

$$R_{\mathrm{p}} = \frac{\sum_a R_a M_a}{\sum_a M_a},$$

where M_a is the molecular mass of residue a. Additionally, the partial specific volume of the protein, ν_{p}, is calculated as the mass weighted partial specific volume, ν_a, of the contributing amino acids,

$$\nu_{\mathrm{p}} = \frac{\sum_a \nu_a M_a}{\sum_a M_a}.$$

Finally, by applying the Lorentz–Lorenz formula, an estimate of the refractive index of the protein is

$$n = \sqrt{\frac{2R_{\mathrm{p}} + \nu_{\mathrm{p}}}{\nu_{\mathrm{p}} - R_{\mathrm{p}}}}.$$

Using the molar refraction of each amino acid reported by McMeekin[15], and the corresponding partial specific volume reported by Cohn[16], the typical refractive index for our IDP is $n_{\mathrm{prot}} = 1.514$.

Due to the electrostatic repulsive forces discussed earlier, the protein can be assumed to have a rigid rod conformation when attached to the gold (Figure 4a). We estimate the volume of the protein as a rectangular box with a square footprint of side length 1.25 nm and a height of 20.0 nm. For simplicity, we will assume each structure sits on a grid, each occupying one corner of a 2.5- × 2.5-nm square (Figure 4b). The interstitial space will be filled with water. A simple estimate of the total effective refractive index of the entire sample chamber, $n_{\mathrm{eff},1}$, has been established by Jung et al.[17] for the Kretschmann geometry. The SPR signal is the result of the interaction of the evanescent field with the refractive index of the sample. For $\lambda = 633$ nm, the penetration depth of this field is $\delta \approx 100$ nm and the intensity decays as $e^{-2y/\delta}$. The effective refractive index is determined by weighting the local refractive index by the intensity along the perpendicular distance from the gold surface. For our example, the first 20 nm have the volume-weighted refractive index of the water and protein, and

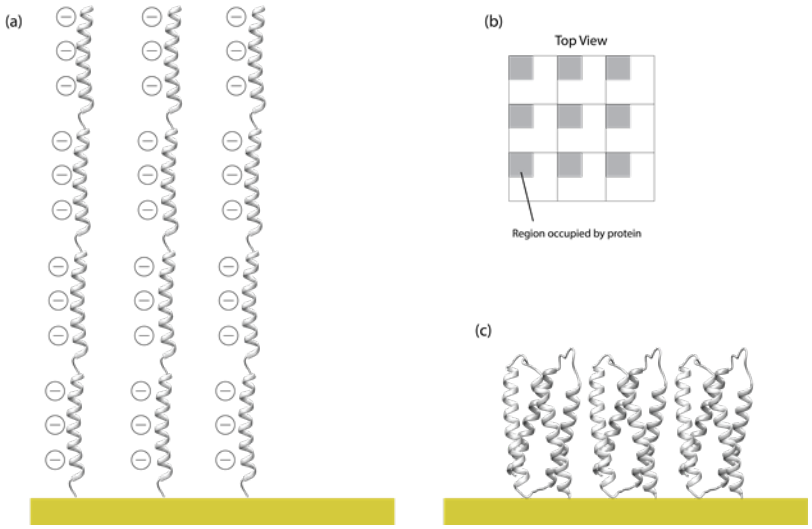

Figure 4. (a) Extended ligand conformation attached to gold film. (b) Top view of protein array where shaded areas indicate surface area occupied by a single protein. (c) Folded ligand upon binding to an analyte (not pictured).

farther out has the refractive index of water alone,

$$n_{\mathrm{eff},1} = \frac{2}{\delta}\left\{\int_0^{20}\left(0.25n_{\mathrm{prot}} + 0.75n_{\mathrm{w}}\right)e^{-2y/\delta}\,dy + \int_{20}^{\infty} n_{\mathrm{w}}e^{-2y/\delta}\right\} = 1.3553$$

Here, $n_{\mathrm{w}} = 1.33$, the refractive index of water.

Once the target analyte is introduced the protein will fold into a rigid structure at the surface of the gold, occupying the entire area of the 2.5- × 2.5-nm square with a height of 5 nm (Figure 3c). Similarly, the effective refractive index can be calculated,

$$n_{\mathrm{eff},2} = \frac{2}{\delta}\left\{\int_0^{5} n_{\mathrm{prot}}e^{-2y/\delta}dy + \int_5^{20} n_{\mathrm{w}}\,e^{-2y/\delta}dy\right\} = 1.3634.$$

This substantial increase in the effective refractive index upon ligand binding will result in a 0.77° increase of the angle of minimum reflectance, almost eighty times the typical SPR signal obtained for antibody/antigen interaction studies.

This calculation did not account for the charged residues on the IDP, and should be considered a lower limit to the effect of the conformational change on the refractive index. The carboxylate groups of the charged protein will contribute significantly to the polarizability of the structure, increasing the effective refractive index above the gold film. Additionally, strong image charges will be induced on the gold film, and may act as a strong perturbance to the resonance frequency of surface plasmons.

2.2 Plasmonic metasurface design and fabrication

Although the analysis began by assuming that the device was configured in the Kretschmann geometry and operated in reflection mode, in the final analysis, the equations describing the change in refractive index caused by the change in protein conformation are not explicitly dependent upon the overall geometry of the device. Thus, we are free to consider other geometric configurations, including transmission-based systems. A transmission-based device has a simpler, easier-to-align, and more robust optical path than a reflection-based system. Thus, for the experimental implementation of the device, we have chosen to develop plasmonic chips which are capable of operating in transmission mode.

Computationally, the easiest metasurface structure to employ in simulations of optical properties is a periodic array of rectangular wires on a dielectric substrate, as shown in Figure 5. The substrate is a fused silica wafer (n = 1.48), which is transparent in the visible, to allow the device to operate in transmission mode. The wire grating is made of gold, in anticipation of using standard thiol chemistry to attach the engineered proteins directly to the metasurface, to maximize the enhancement in the SPR shift. The metasurface is fully immersed in a superstrate, which also fills the grooves between the gold wires, and is assumed to have the same refractive index as water.

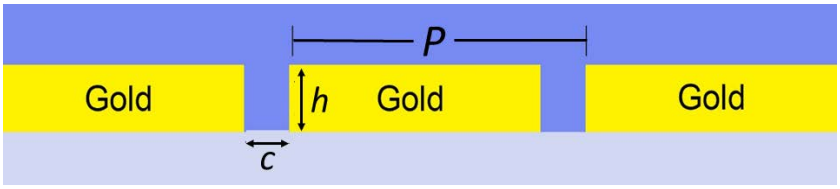

Figure 5. Plasmonic structure, modeled as a grating which is periodic in one dimension. Rectangular metallic gold wires extend into and out of the cross-sectional perspective. The superstrate is a dielectric fluid that fills the grooves between gold wires, and the substrate is a dielectric material.

Preliminary simulations were performed using proprietary software. To maximize the shift in the SPR resonance upon binding, three geometric parameters of the structure were allowed to vary: the gold wire thickness (h); the wire-to-wire period (i.e., the period or pitch of the grating) (P); and the gap between gold wires (c). These simulations indicated that the optimal change in SP transmission in response to the binding of target molecules occurs when the period of the grating P = 630 nm, the height h = 50 nm, and the groove width is 420 nm.

To model a binding event, a 20-nm thick layer atop the gold film within the superstrate, which was initially assumed to be pure water (n = 1.34), experiences an increase in the index of refraction (to n = 1.38), as the protein folds into a denser conformation near the gold surface. The changes are similar to what is expected even with the binding of very small molecular targets, such as heme. Figure 6 illustrates the change in transmission for a grating with the optimized dimensions described above, before and after a small fraction of the attached proteins undergo the model binding event. The predicted change is of a magnitude which should be easily measurable by standard, commercially available silicon photodetectors. Furthermore, a plasmonic structure capable of detecting even this small index change, should be capable of detecting larger target molecules, such as proteins or even viral or bacterial pathogens, which should induce a larger refractive index change upon binding.

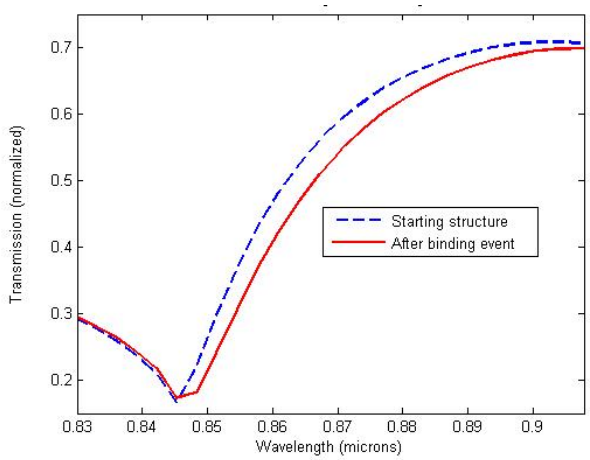

Figure 6. Transmission Curves before (Blue Dashed Line) and after (Red Solid Line) a Minute Amount of Binding Events

More-detailed simulations of the optical transmission through the gratings before and after binding were performed using COMSOL Multiphysics RF Module in the frequency domain. Given the geometry of the grating design, a two-dimensional study was performed, which significantly reduced computation time. The left and right walls were assigned periodic Floquet boundary conditions (i.e., periodic boundary conditions). The top and bottom walls were

assigned as periodic ports. With both in-plane and out-of-plane diffractive orders calculated by COMSOL, there were five ports for the top and five for the bottom. As the actual implementation of this system will use polarized light, we concerned ourselves only with *p*-polarized light (TM polarization) incident from the bottom port. The period of the structure is 630 nm. The height of the upper and lower boxes (with index of refraction of 1.34) are 1.5 times the incident wavelength (~880 nm) in the particular medium to ensure we are away from near-field effects when measuring *S* parameters.

The grating structures that were simulated in COMSOL are shown in greater detail in Figure 6a and b. Figure 6 shows a cross-section of the structure prior to a molecular binding event. The gold is the wire, purple is the glass substrate, and the grey grooves are water, as is the top superstrate in pale blue. The green is the protein layer that was added across the entire width of the unit cell for convenience, even though its effect is most important adjacent to the gold wire (see Figure 8). Prior to the binding event, the protein is in an elongated state, ~40 nm in thickness, as shown in Figure 7a. After the binding event, the protein folds and is only ~5 nm thick, as shown in Figure 7b.

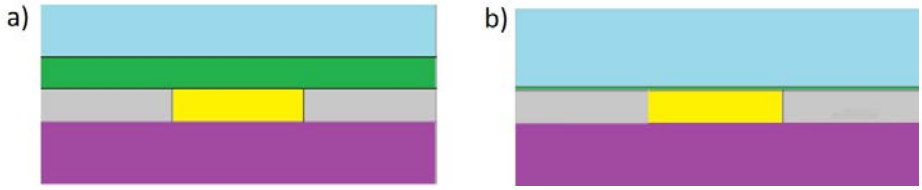

Figure 7 a). Close up of the modeling geometry of grating a) prior to binding and b) after binding. From top to bottom: superstrate (blue, n = 1.348), protein (green, before, n = 1.348, h = 40 nm; after, n = 1.388, h = 5,10, or 20 nm), dielectric grating lines (grey, n = 1.34), gold lines (yellow, n and k from Palik), substrate (purple, n = 1.4832)

Figure 8 is an electromagnetic field intensity map of the SP fields along the grating. The SP fields are exceptionally high and localized near the surface of the gold wire. Thus, the SP field is most concentrated in the same area of the device where the most pronounced change in refractive index occurs during target binding, resulting in the extreme sensitivity of SPR detection.

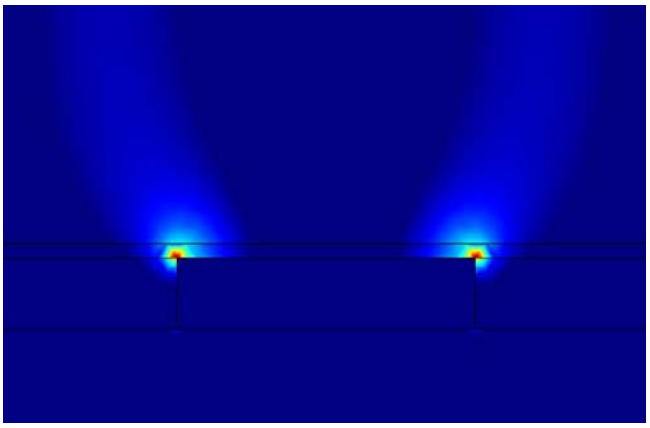

Figure 8. Field enhancement above the gold surface at resonant frequency after binding, at a wavelength corresponding to the lowest observed transmission point from the "post-bind 10-nm layer" curve in figure 7

As the protein layer (n = 1.388) is compressed, it is displaced by water (n = 1.348), changing the transmission, as shown in Figure 9. The change in transmission of normal-incidence 855-nm light is calculated to be at least 7%, and the greater the thickness of the bound protein layer (for instance, if a larger target molecule is bound), the greater the change in the transmission. Even a 7% change is easily detectable using commercially available optical components.

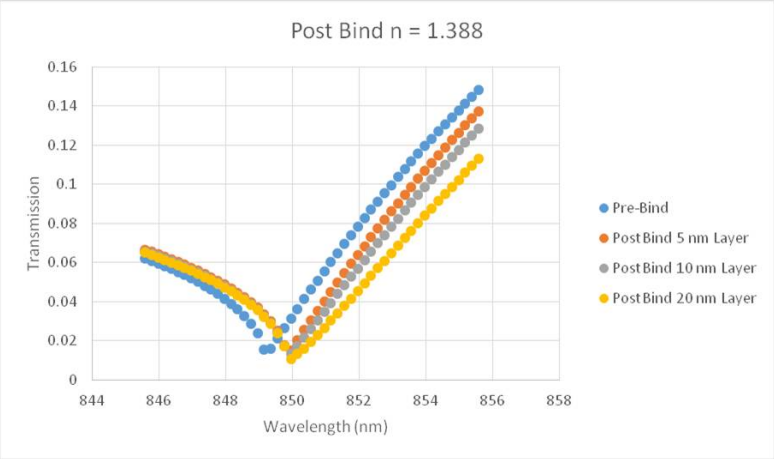

Figure 9. Transmission of grating as a function of wavelength before and after binding; transmission was measured using the *S* 2,1 parameter (i.e., 0th-order transmission); index of refraction is $n = 1.388$, and thickness of bound protein layer is 5, 10, or 20 nm

Taken together, these simulations indicate that a dramatic enhancement in SPR is expected at the surface of protein-bearing gold grating metasurfaces with dimensions which are easily achievable using standard complementary metal-oxide-semiconductor (CMOS) fabrication techniques. To experimentally test these predictions, we have developed a fabrication process for the optimized structure for the plasmonic grating structures onto which the proteins are to be bound. This approach, outlined in Figure 10, uses a liftoff process to produce a gold film, with a grating pattern of alternating rectangular lines and spaces, on the surface of a fused silica substrate.

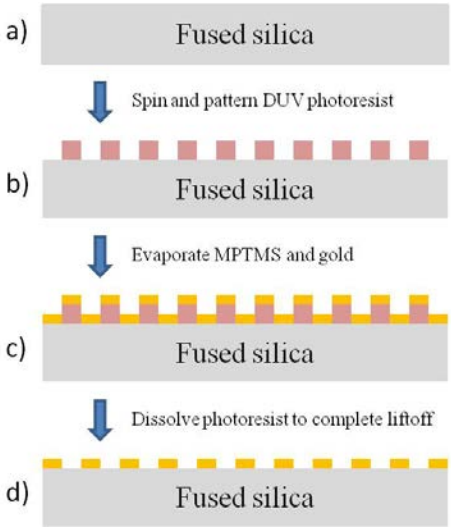

Figure 10. Fabrication process for gold metasurface grating

First, the back side of the fused silica wafer was sputter-coated with a thin layer of chromium, to enable the exposure tool to detect the transparent substrate. Next, the top side of the wafer was spin-coated with an antireflective coating ARC® DS- K101 (Brewer Science Inc.,Rolla, MO), and a deep ultraviolet (DUV) negative tone photoresist, UVN®30 (MicroChem Corp., Newton MA), which were lithographically patterned (Figure 10b). The exposure was performed at 248 nm using a DUV stepper (ASML Holding NV, Veldhoven, Netherlands). Following a post-exposure bake on a hotplate at 95 °C for 90 s, each wafer was developed in AZ®726 MIF (MicroChemicals GmbH, Ulm, Netherlands). Next, a monolayer of (3-mercaptopropyl)trimethoxysilane (MPTMS) (Gelest Inc. ,Morrisville PA) was deposited from the vapor phase, to act as an adhesion promoter for a 50-nm thick layer of gold, which was immediately thereafter evaporated onto the surface (Figure 10c). Finally, the wafer was soaked overnight in an organic solvent, Microposit™

Remover 1165 (MicroChem Corp, Newton MA) to dissolve the remaining photoresist, removing with it the excess gold outside the desired patterns (Figure 10d). Any remaining DS-K101 was removed by soaking the wafer in AZ®726 MIF.

3. RESULTS

Preliminary results of this fabrication process at the resist exposure step (Figure 11b), which investigated a range of UV exposure doses, may be seen in Figure 11. Each square diffraction grating pattern corresponds to a single plasmonic chip. Gratings which are visible from both the top side (Figure 11a) and back side (Figure 11b) of the wafer indicate exposure of the resist throughout its entire depth, which is necessary for a successful liftoff process.

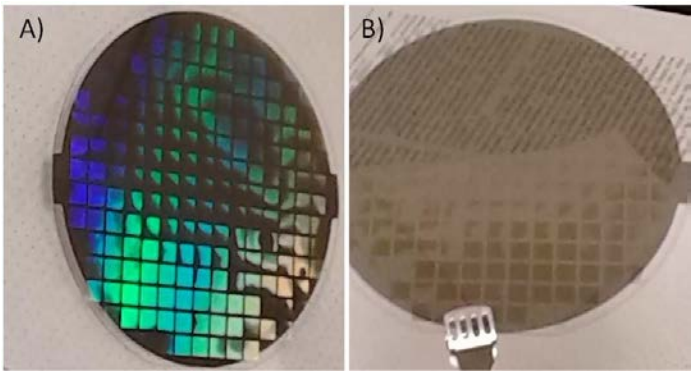

Figure 11 Resist pattern of 220-nm lines in DSK/UVN®30 negative photoresist, viewed from a) top and b) back side of fused silica wafer

The full fabrication process, including the gold deposition and liftoff, was subsequently performed on this wafer. Several grating structures were studied in greater detail by scanning electron microscopy (SEM), viewed both directly from above (as in Figure 12a), and in cleaved cross-section (as in Figure 12b). At 80,000× magnification (Figure 12a), the edges of the gold wires (light grey) look extremely straight when viewed from above. Furthermore, the observed wire width of 195 nm and spacing of 420 nm are extremely close to the targeted values derived from simulations, of 210 nm and 420 nm, respectively. In cross-section (Figure 12b), the measurements of the device dimensions are less reliable, because the sample is at an angle relative to the detector. However, this angle clearly confirms both the complete removal of any residual photoresist and antireflective coating from between the gold wires, and the extreme smoothness of the gold wires themselves, both of which are necessary for a properly functioning plasmonic chip.

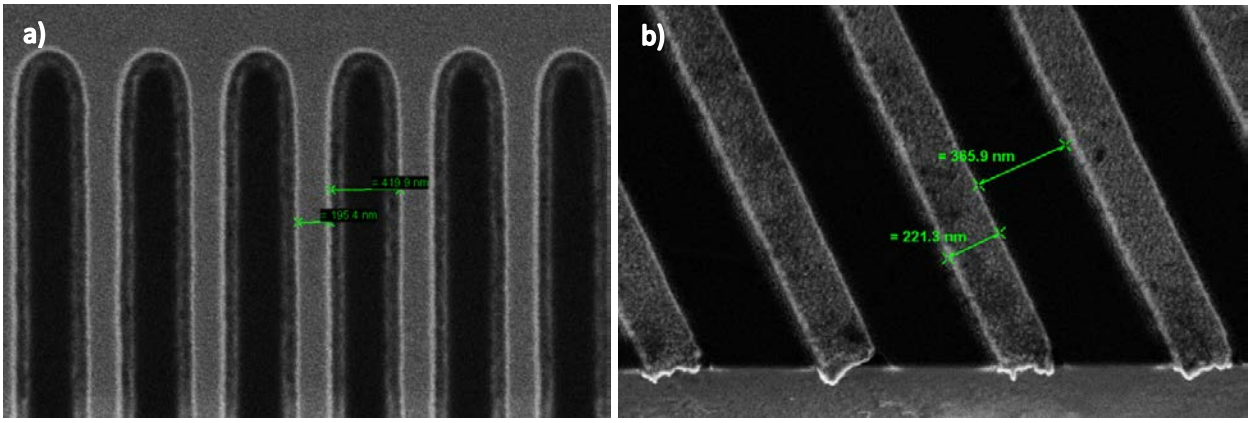

Figure 12 a) Top view and b) cross-sectional SEM view of a gold plasmonic grating pattern on the wafer in figure 11

4. CONCLUSIONS

We have developed the underlying theory and several key components for a proposed handheld biosensor device, which combines proteins designed to undergo extreme conformational changes upon target binding, with plasmonic metasurfaces, to cause an extremely large change in refractive index at the metasurface, thereby causing an orders-of-magnitude enhancement in the SPR signal. The prototype housing has been fabricated, and fitted with the necessary off-the-shelf optical components. The theory relating protein conformational change to refractive index change has been developed, and the engineering of proteins designed to bind specific targets (e.g., heme) is currently in progress. If the proof-of-concept experiments with heme binding demonstrate the predicted SPR enhancement, proteins will be engineered to bind and detect other chemical toxins and pathogens of interest. A successful nanofabrication procedure has been developed for a simple grating structured plasmonic metasurface, and designs for more complex geometries which may enable further enhancements in device sensitivity are in progress.

ACKNOWLEDGEMENTS

This work was supported by the Air Force Civil Engineer Center, through Contract No. FA4819-14-C-0017. This work was performed in part at the Cornell NanoScale Facility, a member of the National Nanotechnology Coordinated Infrastructure (NNCI), which is supported by the National Science Foundation (Grant ECCS-1542081).

REFERENCES

[1] Gopinath, S.C.B., "Biosensing applications of surface plasmon resonance-based Biacore technology," Sensors and Actuators B: Chemical. 150, 722–733 (2010).

[2] Wright, P.E., Dyson, H.J., "Intrinsically unstructured proteins: Re-assessing the protein structure-function paradigm," Journal of Molecular Biology. 293(2), 321–331 (1999).

[3] Dunker, A.K., Lawson, J.D., Brown, C.J., Williams, R.M., Romero, P., Oh, J.S., Oldfield, C.J., Campen, A.M., Ratliff, C.M., Hipps, K.W., Ausio, J., Nissen, M.S., Reeves, R., Kang, C.-H., Kissinger, C.R., Bailey, R.W., Griswold, M.D., Chiu, W., Garber, E.C., and Obradovic, Z., "Intrinsically disordered protein," Journal of Molecular Graphics & Modelling. 19(1), 26–59 (2001).

[4] Dyson, J. H., Wright, P. E., "Intrinsically unstructured proteins and their functions," Nature Reviews. Molecular Cell Biology. 6(3), 197–208 (2005).

[5] Negron, C., Fufezan, C., Koder, R.L., "Geometric constraints for porphyrin binding in helical protein binding sites," Proteins-Structure Function and Bioinformatics. 74(2), 400–416 (2009).

[6] Nanda, V., Koder, R.L., "Designing artificial enzymes by intuition and computation," Nature Chemistry. 2(1), 15–24 (2010).

[7] Mutter, A.C., Norman, J.A., Tiedemann, M.T., Singh, S., Sha, S., Morsi, S., Ahmed, I., Stillman M.J., Koder, R.L., "Rational design of a zinc phthalocyanine binding protein," Journal of Structural Biology. 185(2), 178–185 (2014).

[8] Hemmings, H.G. Jr., Nairin, A.C., Aswad, D.W., Greengard, P., "DARPP-32, a dopamine- and adenosine 3':5'-monophosphate-regulated phosphoprotein enriched in dopamine-innervated brain regions. II. Purification and characterization of the phosphoprotein from bovine caudate nucleus," The Journal of Neuroscience. 4(1), 99–110 (1984).

[9] Gast, K., Damaschun, H., Echert, K., Schulze-Forster, K., Maurer H.R., Muller-Frohne, M., Zirwer, R., Czarnecki, J., Damaschun, G., "Prothymosin alpha: a biologically active protein with random coil conformation," Biochemistry. 34(40), 13211–13218 (1995).

[10] Weinreb, P.H., Zhen, W., Poon, A.W., Conway, K.A., Lansbury, P.T. Jr., "NACP, a protein implicated in Alzheimer's disease and learning, is natively unfolded," Biochemistry. 35(43), 13709–13715 (1996).

[11] Uversky, V.N., Gillespie, J.R., Fink, A.L., "Why are 'natively unfolded' proteins unstructured under the physiological conditions?" Proteins: Structure, Function, and Bioinformatics. 41(3), 415–427 (2000).

[12] Ebbesen, T.W., Lezec, H.J., Ghaemi, H.F., Thio, T., Wolff, P.A. "Extraordinary Optical Transmission Through Sub-Wavelength Hole Arrays" Nature, 391(6668) 667–669 (1998).

[13] Kretschmann, E., Raether, H., "Radiative Decay of Non Radiative Surface Plasmons Excited by Light," Zeitschrift für Naturforschung A, 23, 2135–2136 (1968).

[14] McMeekin, T.K., Groves, M.L., Hipp, N.J., "Refractive indices of amino acids, proteins, and related substances," Amino Acids and Serum Proteins. American Chemical Society. Chapter 4, 54–66 (1964).

[15] McMeekin, T.L., Wilensky, M., Groves, M.L., "Refractive indices of proteins in relation to amino acid composition and specific volume," Biochemical and Biophysical Research Communications, 7(2) 151–156 (1962).

[16] Cohn, E.J., Edsall, J.T., "Density and apparent specific volume of proteins," Proteins, Amino Acids and Peptides, Van Nostrand–Reinhold, 370–381 (1943).

[17] Jung, L.S., Campbell, C.T., Chinowsky, T.M., Mar, M.N., Sinclair, S.Y., "Quantitative Interpretation of the Response of Surface Plasmon Resonance Sensors to Adsorbed Films," Langmuir, 15(19), 5636–5648 (1998).